Liver Function as an Engineering System

William Ashworth
Centre for Process Systems Engineering, Dept. of Chemical Engineering, University College London, London WC1E 7JE, U.K.

Institute for Liver and Digestive Health, Division of Medicine, University College London, Royal Free Campus, London NW3 2PF, U.K.

COMPLEX (Centre for Mathematics and Physics in the Life Sciences and Experimental Biology), University College London, London WC1E 6BT, U.K.

Carlos Perez-Galvan
Centre for Process Systems Engineering, Dept. of Chemical Engineering, University College London, London WC1E 6BT, U.K.

Nathan Davies
Institute for Liver and Digestive Health, Division of Medicine, University College London, Royal Free Campus, London NW3 2PF, U.K.

Ian David Lockhart Bogle
Centre for Process Systems Engineering, Dept. of Chemical Engineering, University College London, London WC1E 7JE, U.K.

COMPLEX (Centre for Mathematics and Physics in the Life Sciences and Experimental Biology), University College London, London WC1E 6BT, U.K.

DOI 10.1002/aic.15292
Published online June 30, 2016 in Wiley Online Library (wileyonlinelibrary.com)

Process Systems Engineering has tackled a wide range of problems including manufacturing, the environment, and advanced materials design. Here we discuss how tools can be deployed to tackle medical problems which involve complex chemical transformations and spatial phenomena looking in particular at the liver system, the body's chemical factory. We show how an existing model has been developed to model distributed behavior necessary to predict the behavior of drugs for treating liver disease. The model has been used to predict the effects of suppression of de novo lipogenesis, stimulation of β-oxidation and a combination of the two. A reduced model has also been used to explore the prediction of behavior of hormones in the blood stream controlling glucose levels to ensure that levels are kept within safe bounds using interval methods. The predictions are made resulting from uncertainty in two key parameters with oscillating input resulting from regular feeding. © 2016 The Authors AIChE Journal published by Wiley Periodicals, Inc. on behalf of American Institute of Chemical Engineers *AIChE J*, 62: 3285–3297, 2016
Keywords: mathematical modeling, biomedical engineering, systems biology, medical, control

The liver, its regulation, and its diseases

Why systems engineering of the liver?

Systems Engineering is the discipline of the management of complex engineering systems over their whole life cycle. Process Systems Engineering is the study of complex process engineering systems involving chemical and physical change. Prof Roger Sargent was a pioneer from the 1950s in seeing the potential that computers could have to revolutionize the way that we tackled these problems.[1] He also saw the way Chemical Engineering was broadening its base into molecular and biological systems to improve manufacturing.[1,2]

The liver is one part of a very complex processing system which ensures that all parts of the body receive the energy and nutrients that they need, that waste products are removed efficiently from the various streams, and that short and long term well being are maintained. It is the body's central chemical processing organ. Considering the liver system as one which controls chemical and physical change within the body, particularly of nutrition, makes it a legitimate area of study for Process Systems Engineers. A number of Chemical Engineers have also contributed to the use for Process Systems Engineering to a range of medical applications. Bogle[3] reviews recent

Correspondence concerning this article should be addressed to D. Bogle at d.bogle@ucl.ac.uk.

contributions in the area and Refs. 4–8 give some further examples and perspectives from the Process Systems Engineering community. Many others have contributed to the area often known more broadly as Systems Biology, and Systems Medicine when clinical objectives are to the forefront.

The liver functions as part of a system involving many organs of the body but with particularly strong interactions with the pancreas, the blood stream, and the body fat known as adipose tissue.[9] The liver system performs a number of functions: regulating the level of glucose and cholesterol in the blood, removing toxins (such as alcohol) from the body, releasing bile among others. Fluid flow principles govern the blood flow behavior providing nutrients to the liver cells which receive entities through the cell membrane which in turn affect the cell metabolism and its signaling pathways.

This can be considered in the way that complex chemical manufacturing systems are treated. Each organ can be treated as a "unit operation." The processes are more complex, particularly the biochemistry. Many in the life sciences also recognize the role that modeling can play in the future of medicine (see for example Refs. 10–12). The elements of the system lifecycle of engineering projects have similar phases in medicine. Modeling of systems is often undertaken to clarify our understanding of the elements that drive a complex system be it chemical or medical. Analysis of a system can best be seen as making a prognosis, design as devising a therapy, and operations as managing a process designed to maintain well-being of a patient or managing a disease condition.[4] The modeling task develops increasing understanding of the systems involved and new model requirements for new functionality. Here, the need for modeling variation in liver cell function across the microstructure of the liver is reported using distributed systems modeling.

There is considerable uncertainty in both parameter values and causation and Chemical Engineers have developed and used Process Systems Engineering techniques to handle uncertainty (see review of optimization under uncertainty[13]). In this article we show how one particular technique, interval methods, can be used to tackle uncertainty in complex medical systems problems. To control normal body function the liver is a key organ in the regulation of the level of glucose in the blood stream, a process known as glucose homeostasis. The body needs the concentration of glucose in the blood to be between limits. Above the upper limit is a condition known as hyperglycaemia while below the lower limit, hypoglycaemia a deficiency of glucose in the bloodstream.

Glucose homeostasis is mediated by the production of hormones in the pancreas which stimulate the storage of glucose as glycogen if there is excess glucose and the breakdown of glycogen when the blood glucose level drops. Figure 1 shows a very simplified "flowsheet" for glucose storage in liver.

Diseases of the liver system

As the liver system is so central to the chemical functioning of the body it has a key role in disease and detoxification. There is a huge amount of data on liver function and much has been assembled in in a comprehensive database called Liverbase.[14] Liver diseases can arise due to a wide range of causes including toxins such as alcohol or paracetamol, viral infection, and metabolic dysregulation. In particular, here we discuss the liver damage resulting from the build-up of fats in the liver (steatosis) known as non-alcoholic fatty liver disease (NAFLD), which can result in inflammation (hepatitis), scar tissue formation (fibrosis), and irreversible cell death (cirrhosis). Excess liver fat is additionally strongly associated with the development of type 2 diabetes mellitus.[15,16] This is a condition where the liver cells become insulin resistant and no longer store glucose as glycogen, distinguished from type 1 diabetes in which the pancreas fails to produce insulin.

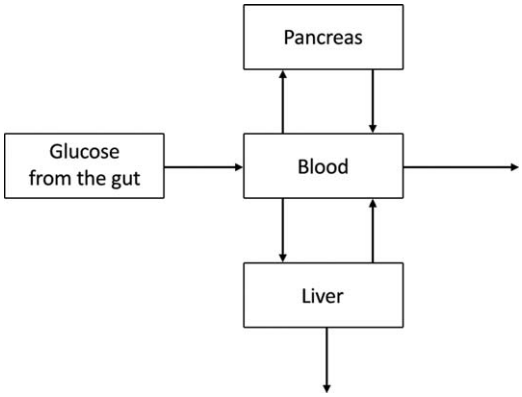

Figure 1. A simple version of the liver system.

The majority of liver diseases affect cells more severely in different parts of the liver microstructure more than others, including viral infections such as viral hepatitis, alcohol related disease, paracetamol poisoning, and NAFLD.[17] The damage resulting from paracetamol and alcohol tends to affect cells in the low oxygen venous parts of the liver microstructure where detoxification enzymes are upregulated. As discussed below, NAFLD also tends to damage these cells most severely. Meanwhile, the more oxygenated arterial regions of the liver microstructure are most susceptible to viral hepatitis.

Models for type 1 diabetes require the prediction of behavior of insulin production in the pancreas. For type 2 diabetes any model will need to involve parts of the metabolism which are catalyzed by insulin and ways of changing the kinetics of those reactions to reflect increasing resistance. In this article we discuss a model which also includes aspect of liver lipid metabolism, allowing us to investigate the build-up of fats across the liver microstructure and its relationship with insulin resistance.

Modeling and Analysis of Basic Liver System Function

Since diabetes is an important disease there have been a number of modeling efforts directed at specific aspects. Balakrishnan et al.[18] reviewed blood glucose models for type 1 diabetes, Li and Chan[19] for liver toxicity and Subramanian et al.[20] for drug-induced liver injury. Galvanin et al.[21] have devised an approach to determine an optimal set of clinical tests to identify diabetes models. Many engineers have explored the use of real time control for managing diabetes: Finan et al.[22] explored the effect of exciting a range of inputs on empirical dynamic models for type 1 diabetes to explore the sensitivity and safety of use, Zavitsanou et al.[23] modeled the insulin delivery system, Semizer et al.[24] compared control algorithms for virtual patients with an artificial pancreas and Percival et al.[25] developed a practical control approach in an artificial pancreatic beta cell. Liu et al.[26,27] modelled the dynamics of the insulin signaling pathway while Cardenas and Goldbeter[28] explored a specific switch in the metabolism, between glucose phosphorylase and glycogen synthase. Life scientists have developed great expertize in understanding and modeling metabolic signaling behavior. Klingmuller et al.[29]

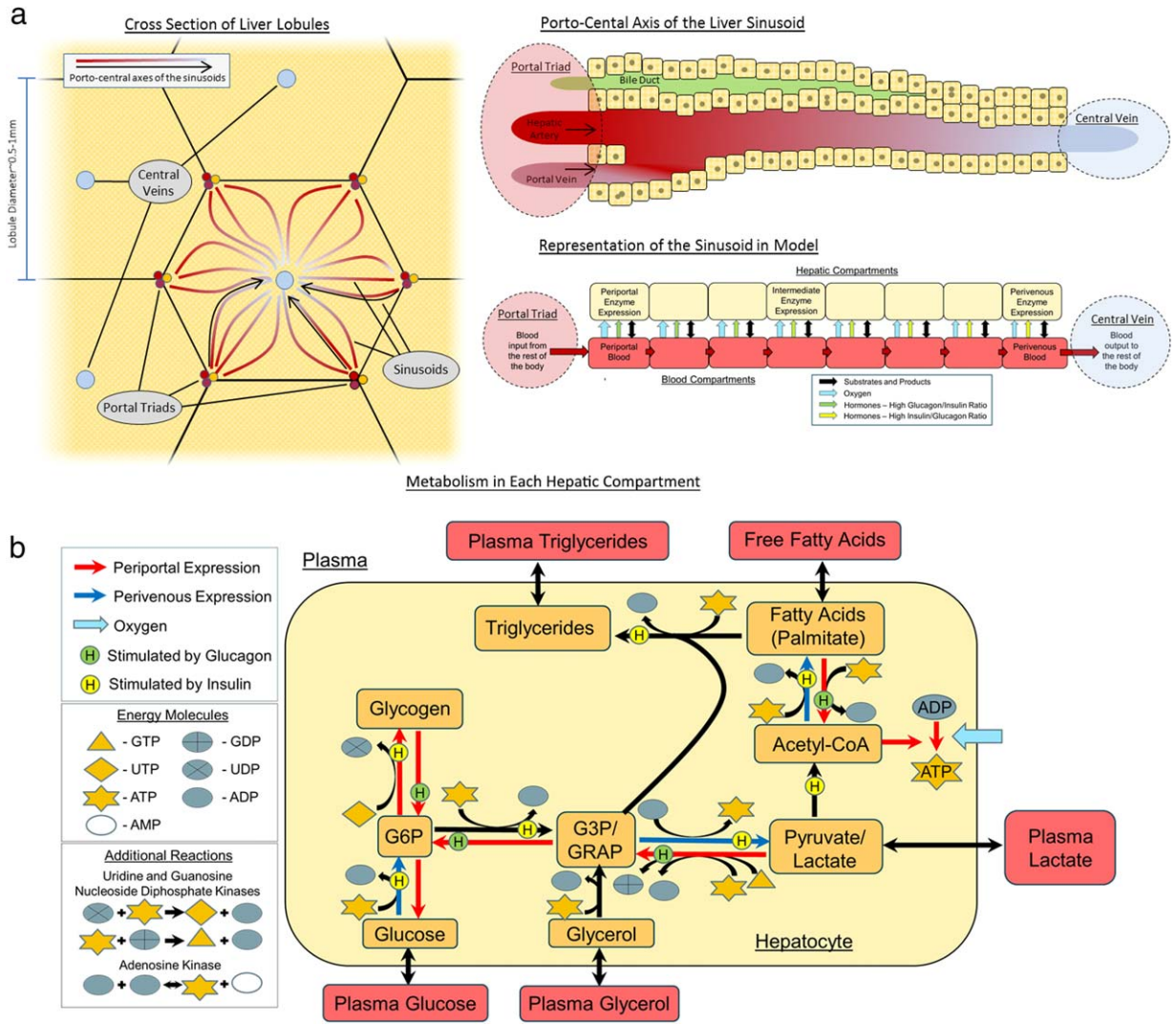

Figure 2. (a) Treating the 1D porto-central axis of the sinusoid as the repeating unit of the liver. (b) The processes and metabolites included in each hepatic compartment.

[Color figure can be viewed in the online issue, which is available at wileyonlinelibrary.com.]

report on comprehensive *in vitro* experiments for cultured hepatocytes as a precursor for modeling of signal transduction pathways while Wu et al.[30] used discrete models for a dynamic analysis.

Kim et al.[31] developed a mathematical model of the whole body metabolism to predict homeostasis using hormonal control. Their model simulations were validated using data from human exercise studies and was able to predict dynamic changes in glycogenolysis and gluconeogenesis, two key hormonal processes.

Bringing together many aspects of this complex system benefits from assembling models from a wide range of sources. Hetherington *et al*. developed a composite model to predict glucose homeostasis. The model consists of seven models drawn from different sources incorporated into a model management system which allows data and models to be updated as improved information becomes available.[32–34] The model was able to predict the naturally occurring oscillations, known as ultradian oscillations. Previously these were thought to be produced by the pancreas alone but the model demonstrated that this is in fact a systems phenomenon resulting from interactions between the pancreas and the liver. The model was used as a tool to aid understanding but also for analysis using a detailed sensitivity analysis to explore what are the key controlling parameters in the model.[35]

All of these chemical pathways are linked together and also to many other metabolic functions within the body. No model is able to deal with all conditions or circumstances. Hangos and Cameron[36] discuss about the need for being clear about the purpose of any model in preparation for model development. In this article we expand the functionality of the Hetherington et al. model to embrace new purposes all of which are related to the chemical functioning of the liver system. Hetherington et al.[32] used the "middle out" approach recommended by Noble[10] for physiological modeling. While stand-alone models for aspects of liver system function may be possible, because of the complex interconnectivity of much of the chemical pathways involved in the modulation of glucose we have taken the approach of building new elements into the model as new objectives are set. The variation of hepatocyte function across the liver plate is known to affect toxicology and drug behavior (e.g., Jungermann et al.[37]) which requires distributed modeling.

Process Systems techniques could be used in a number of ways but this article focuses on just two aspects. The first is a

development of the model to incorporate distributed behavior by relaxing the assumption that hepatocyte cells are homogeneous. This is known as zonation and is discussed in the following section. There is considerable uncertainty in data and behavior which it will be important to be able to incorporate if we are to be able to determine actions while guaranteeing that the glucose level will definitely remain within safe bounds. We have been using interval techniques to obtain bounded behavior and the subsequent section outlines an approach to explore the behavior of the system subject to uncertainties in the parameters.

Modeling and Design for Distributed Behavior

Zonated effects

Zonation is the name given to the heterogeneity between liver cells depending on their position along the capillaries supplying them with blood. On the microscale, liver cells are organized into tessellating columns with hexagonal cross-sections known as lobules (Figure 2a). The portal vein supplies nutrient-filled blood from the digestive system while the hepatic artery supplies oxygenated blood from the lungs. The portal vein and hepatic artery split into branches which pass along the outer corners of each lobule along with the bile ducts (collectively known as the portal triad). Blood leaves the lobules through the hepatic central veins which pass through the centre of each lobule. Capillaries, called sinusoids, pass between each portal triad and central vein supplying the surrounding cells with blood (Figure 2a). As blood passes through the liver sinusoids, the concentrations of hormones, oxygen and nutrients fall while the concentration of liver products increase (Figure 2b). To compensate, liver cells (hepatocytes) show marked variation in enzyme expression and function depending on their position along the sinusoid, known as zonation. Zonation is seen in the enzymes mediating almost all liver processes.

When considering glucose and lipid metabolisms, the major motivation for zonated enzyme expression is to allow sufficient production of adenosine triphosphate (ATP) in cells near the central vein (pericentral/perivenous), where the blood oxygen concentration is markedly reduced. ATP effectively acts as the molecular unit of energy utilized by enzymes to drive forward reactions. Energy is released when ATP is reacted with water and split (hydrolysed) to give adenosine diphosphate (ADP) and a free (inorganic) phosphate (P_i). However, since relatively little cellular ATP exists at any point in time (about 0.2 mol in the whole body), constant synthesis is required. ATP is predominantly produced by the enzyme ATPsynthase using recycled ADP and P_i as substrates. The process requires oxygen to produce water (H_2O) from the release of potentially damaging protons (H^+). The reduced supply of oxygen in pericentral cells forces them to downregulate this oxidative ATP synthesis through ATP synthase to avoid damage resulting from free protons. To compensate for this, the most ATP intensive processes are restricted to oxygen rich cells near the portal triad (periportal). Meanwhile, pericentral cells specialize in the conversion of glucose to pyruvate (glycolysis), which produces a small amount of additional ATP without the requirement for oxygen. This pyruvate is either released into the blood as lactate or converted to fatty acids (lipogenesis). Due to their oxygen rich environment, periportal cells specialize in the conversion of lactate back to glucose (gluconeogenesis), which consumes ATP. They also generate a higher proportion of their energy through oxidation of fatty acids, where pericentral cells use a higher proportion of glucose via glycolysis.

Due to the marked differences across the sinusoid, particular regions of the sinusoid have been shown to be more susceptible to damage in numerous liver diseases including drug and alcohol abuse, viral infection and metabolic disorders. In the case of NAFLD, fat build-up (steatosis) and the resulting damage have been shown to occur most severely toward the pericentral end of the sinusoid.[38–41] Although this is extensively referred to in the literature, few investigators attempt to understand the metabolic differences leading to pericentral-centered steatosis or the implications of differences across the sinusoid in pharmacological treatment. This is largely because experiments investigating changes in individual regions of the sinusoid are time consuming and complex compared with assessing bulk changes in tissue homogenate. However to fully understand the development of the disease and to optimize pharmacological interventions, we must develop an understanding of the zone-specific changes.

In our studies, a computational model of metabolism across the liver sinusoid was built, integrating existing knowledge of differences in enzyme expression across the sinusoid. This was firstly used to simulate high fat intake and insulin resistance to study the build-up of liver fat in NAFLD.[42] Secondly it was used to identify key processes of inter-individual variation in susceptibility to NAFLD and its pattern of development.[42] Finally, in ongoing work, in combination with cell culture studies, the model is being used to test the effects of various potential pharmacological interventions. It is hoped that these predictions will aid understanding and allow for more targeted future experimentation. Here we review the structure of the model and its use in simulating the build-up of liver fats in NAFLD, before using the model to test the pertinence of two key drug targets for clearing liver steatosis to demonstrate its use in assessment of pharmacological targets.

Zonated model of glucose and lipid metabolism

Model Structure. Conventional two compartment models of hepatic metabolism treat the liver as a single mass of hepatocytes interacting with a compartment representing blood. For many applications this is sufficient for representing the bulk effects of liver on the blood. However, a model of this form cannot be used to study the heterogeneity in hepatic enzyme expression and blood supply. Instead, following the structure suggested by Ohno et al.[43] the one dimensional axis from the portal triad to the central vein of the hepatic sinusoid (porto-central axis) was used as the repeating unit of the liver rather than the individual hepatocyte (Figure 2a). Hepatocytes, and the nearby blood, were split into compartments according to their position along the porto-central axis, with blood flow from the portal trial to the central vein. Minimal representations of essential processes in blood glucose and lipid regulation which occur outside the liver act on an additional large compartment representing blood in the rest of the body. These include gut triglyceride synthesis, adipose triglyceride breakdown (lipolysis), adipose lipogenesis, pancreatic hormone release, and oxygen input from the lung.[42] Dietary intake of glucose and lipid is introduced to this compartment. Alternatively, the recirculation can be removed and the model can be used to study the input of plasma with constant metabolite, hormone and oxygen concentrations into the sinusoid.

Splitting hepatocytes into compartments in this way allows the inclusion of zonated enzyme expression and changes in blood supply across the sinusoid. When building the model, the effects of altering the number of compartments into which the sinusoid was split was tested: from 3 compartments to 48. For the published simulations, eight compartments were used to match the largest number of compartments used experimentally. No undersampling effects were noted using eight compartments in comparison with 48.

Conversions in the Model. The rates of processes in the model are calculated by multiplying a hormone- and compartment-dependent rate constant by a Hill function dependent on the substrates and allosteric activators and inhibitors. For example, for a process with two substrates, S_1 and S_2, which was allosterically inhibited by molecule i, the rate would be calculated as:

$$v = \frac{v_x(h)[S2]^{n_{S1}}}{K_M^{S1 n_{S1}} + [S1]^{n_{S1}}} * \frac{[S2]^{n_{S2}}}{K_M^{S2 n_{S2}} + [S2]^{n_{S2}}} * \left(1 - \propto_{inh} \frac{[i]^{n_{inh}}}{K_i^{n_{inh}} + [i]^{n_{inh}}}\right)$$

where $v_x(h)$ is the rate constant in compartment x, under the influence of hormone concentrations h and K_M, n_S, K_i, and n_{inh} are the Michealis-Menten (half occupation) constant, Hill coefficient, inhibition constant and inhibition coefficient, respectively. $\propto_{inh} \leq 1$ determines the maximum inhibition by i. The values of constants were either taken directly from the literature or, where this was not possible, fitted to data looking at hepatic metabolism under different feeding conditions (see Ashworth et al.[42] for more details). In many cases, the processes represented in the model contain several intermediate enzymes and the constants were based on the literature for the rate limiting enzyme in the process. Previous models have represented each individual enzyme separately (e.g., Konig et al.[44]). However, here we focus on key rate limiting enzymes, and those which show variation in activity across the sinusoid.

Hormonal regulation by insulin and glucagon is represented through a hormone-dependent rate constant. Rather than modeling downstream signaling (e.g., as in Hetherington et al.[32]) the effects of the hormones are calculated based on the plasma concentrations. As a result, the form of the equations and parameter values were largely set by comparison with experimental data for plasma concentrations of key metabolites and for hepatic rates, rather than taken directly from the literature as discussed in Ashworth et al.[42].

Finally, the activities of key enzymes vary across the sinusoid. To represent this, the base-value (v_b) for each rate constant was increased or reduced in each compartment according to whether the enzymes mediating each process are known to be upregulated or downregulated in that region of the sinusoid. For the processes represented in this model, a gradient-like change is seen in enzyme activity across the sinusoid. For other processes, such as some of the enzymes involved in cholesterol synthesis or drug detoxification, enzymes are more strongly restricted to one particular region. The upregulation or downregulation of each process in each compartment was based on experimental data for the activities or expression of key enzymes across the sinusoid.[42]

Hepatic Metabolism.

ATP Production. The processes represented in each hepatic compartment are shown in Figure 2b. As discussed, cellular metabolism is centred around ensuring continuous availability of ATP. ATPsynthase is reliant on energy generated from a proton gradient across the mitochondrial inner membrane. To produce this proton gradient, continuous oxidation of acetyl-CoA through the citrate cycle is required to fuel a set of proton pumps in the electron transport chain. Acetyl-CoA is derived from glucose originating from dietary carbohydrates and sugars, free fatty acids (FFAs) originating from dietary fat and some amino acids (protein components). In the model, the citrate cycle, electron transport chain and synthesis of ATP from ADP are represented as a single process with a rate dependent on the cellular acetyl-CoA, ADP, P, and oxygen concentrations.

Glucose Metabolism. Liver cells play a vital role in ensuring blood glucose concentrations remain in a relatively narrow healthy range. The model includes the key processes involved in the hepatic regulation of blood glucose concentrations and in the production of acetyl-CoA from glucose. These include glucose uptake and release, glycogen synthesis and breakdown, glycolysis (glucose → lactate), gluconeogenesis (lactate → glucose), lactate uptake and release, and pyruvate oxidation (acetyl-CoA production from pyruvate/lactate). Additionally, the model includes glycerol uptake (predominantly produced through triglyceride breakdown in adipose tissue) and the production of glycerol-3-phosphate from glycerol, glucose or lactate which is required in triglyceride synthesis.

Fatty Acid Metabolism. The model includes the key processes involved in the production of acetyl-CoA from fatty acids, in fatty acid synthesis and the storage and in the release of excess fatty acids as triglycerides (three fatty acids attached to a glycerol backbone). These include fatty acid uptake, lipogenesis, β-oxidation (fatty acid breakdown to acetyl-CoA), triglyceride synthesis from three fatty acids and a G3P molecule, triglyceride release and lipolysis. In the model, all fatty acids contain eight acetyl-CoA molecules corresponding to palmitate, the most common fatty acid in humans and in dietary intake. It is known that different fatty acids have varying potencies in causing both insulin resistance and in promoting the progression to non-alcoholic steatohepatitis (NASH). Therefore, a project for future work may be to separate the different fatty acids in the model. This would allow us to simulate the possibility of pharmacologically promoting the conversion of fats to less damaging forms, rather than aiming to clear them completely. However, the current work focuses on clearing the build-up of non-specific fats (in the form of triglycerides) without causing problems elsewhere in metabolism.

Inputs and representing NAFLD in the model

To represent daily dietary intake, the model was provided with spiked dietary carbohydrate and fat inputs at 4 h intervals. For moderate carbohydrate and fat intake, the total inputs for each meal were set to match the averages provided per meal in a study performed by Daly et al.[45] (78.1 g of carbohydrates and 22.2 g of lipid per meal) allowing comparison of the model predictions with the measurements made in the study. When simulating this diet an average hepatic fat content toward the low end of the values measured in the US general population by Szczepaniak *et al*. is predicted consistent with simulating a healthy diet.[46] The predicted plasma and hepatic concentrations of the various metabolites were extensively validated against numerous sources of experimental data.[42]

Patients suffering from NAFLD vary across a broad range in their dietary intake and extent of metabolic dysregulation. To account for this, various degrees of insulin resistance were

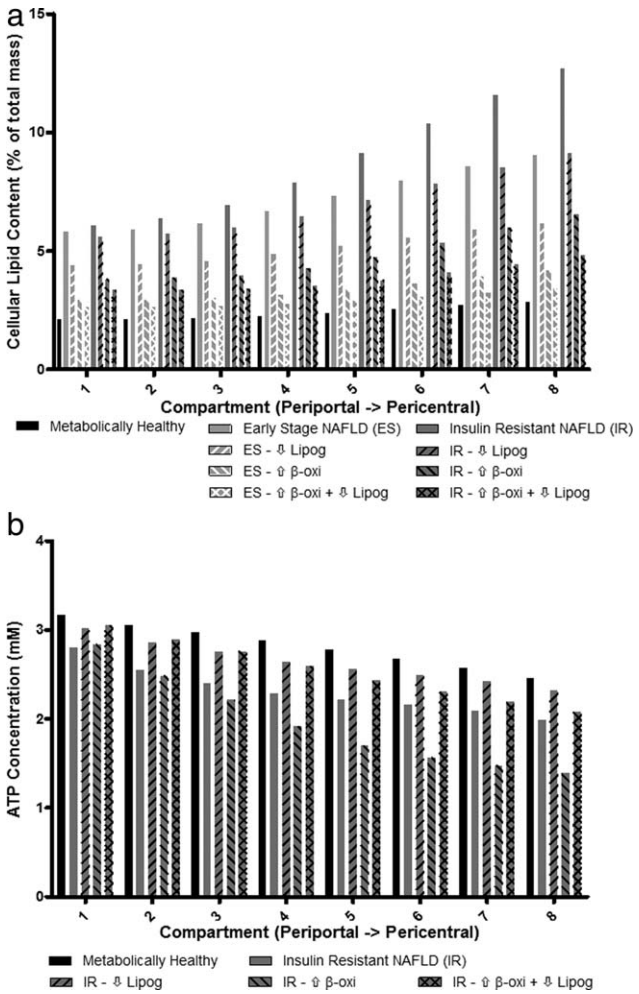

Figure 3. The predicted (a) cellular lipid content (as percentage of cell mass) and (b) ATP concentration across the sinusoid.

simulated with varying fat and glucose intake. The various contributing factors and the development of steatosis across the sinusoid are discussed in detail in Ashworth et al.[42]. Here, we consider two sets of conditions leading to excess liver fat in the model, before considering potential drug targets to remove these fats and restore normal function: first, steatosis resulting from very high intake alone in an otherwise metabolically healthy individual. Since lipid build-up is known to promote insulin resistance, this is likely to be an early stage in NAFLD development. Second, we have considered steatosis arising with only slightly raised fat intake in an individual with severe insulin resistance (1.5% detection). In addition to insulin resistance, the effects of an increase in the lipogenic transcription factor sterol regulatory element-binding protein-1c (SREBP-1c) seen in NAFLD patients *in vivo* were also simulated.[47,48]

When simulating increased dietary fat intake in an otherwise metabolically healthy individual, the increases in hepatic triglyceride concentration (roughly equal to the total lipid content) were relatively moderate. A very high lipid intake diet was used, such that the predicted plasma FFA and triglyceride concentrations reached the high end of those measured experimentally in obese individuals.[49,50] Under these conditions, the predicted hepatic lipid content increased to 7.2% (Figure 3a). An increasing gradient in concentration was predicted across the porto-central axis of the sinusoid consistent with the increased pericentral susceptibility to steatosis seen *in vivo*.

When simulating a severely insulin resistant NAFLD patient, increased dietary lipid intake was predicted to cause a much larger increase in hepatic triglyceride concentrations (Figure 3a). Even when simulating only slightly raised fat intake (22.8 g/meal), the liver fat content increased to 8.9%, compared with 2.5% if the same diet is simulated in a metabolically healthy individual. As with high fat intake, the most severe steatosis was predicted in perivenous cells, consistent with experimental observations. Higher intake diets when simulating insulin resistance were predicted to increase the hepatic lipid content up to the $>20\%$ values at the highest end of those measured experimentally.[46]

In addition to the build-up of lipids in hepatocytes, insulin resistance is associated with a reduction in hepatic glycogen concentrations, leading to hyperglycaemia and type-2 diabetes mellitus (T2DM). This fall in glycogen storage was predicted to be most severe in pericentral cells, consistent with previous experimental studies.[51]

ATP concentrations were predicted to fall when simulating insulin resistance, particularly when combined with raised dietary lipid intake (Figure 3b), as is seen experimentally.[52–56] This was notably more severe in perivenous, than periportal cells. Disruptions to energy metabolism have been suggested as possible mechanisms for the progression of NAFLD to NASH.[57,58] *In vivo*, as NAFLD and NASH develop, loss of function in the oxidative phosphorylation enzymes results in further drops in ATP concentrations.[59] In addition to the problems associated with reduced ATP concentrations, the predicted overactivation of oxidative ATP synthesis may lead to production of damaging reactive oxygen species (ROS), as seen in NAFLD *in vivo*.[59–63]

To avoid hepatic damage and loss of function, any pharmacological intervention must not further reduce ATP concentrations or exacerbate the overactivation of oxidative ATP synthesis. The zone-specificities of many of the metabolic changes highlight the requirement for studying the sinusoid as a whole, rather than homogenized whole tissue alone.

Assessing potential drug targets

Numerous processes in the model provide potential drug targets. Here, as key examples, we focus on hepatic production of fatty acids from acetyl-CoA and oxidation of fatty acids. A full study of the effects of pharmacologically targeting each process will be presented in combination with additional cell culture data testing of predictions in the near future. Pharmacologically stimulating or inhibiting a process was simulated by increasing or reducing its rate constants.

Suppression of de novo lipogenesis. Suppression of *de novo* lipogenesis (blocking the process completely) is predicted to reduce hepatic FFA concentrations across the range of NAFLD stages simulated (Table 1). FFAs are thought to be more potent in causing both hepatic damage leading to NASH and in promoting insulin resistance than fats stored as triglyceride. As a result, the reduction in FFA concentration is likely to reduce lipotoxicity. Furthermore, by preventing cycling between lipogenesis and β-oxidation, suppressing the process increased ATP concentrations to near metabolically normal levels (Figure 3b). It also reduced the overactivation of the oxidative phosphorylation pathways to metabolically normal levels. However, the total liver fat content was predicted to only show a relatively small reduction when simulating either

Table 1. Results for the Predicted Effect of Targeting Lipogenesis and β-Oxidation on Hepatic Triglyceride, FFA and ATP Concentrations and Plasma Triglyceride, FFA, Glucose and Lactate Concentrations When Simulating NAFLD Resulting from High Intake, and from Raised Intake in a Severely Insulin Resistant Individual

	Average hepatic FFA concentration (μM)	Average hepatic ATP concentration (mM)	Average plasma triglyceride concentration (mM)	Average plasma FFA concentration (mM)	Average plasma glucose concentration (mM)	Average plasma lactate concentration (mM)	Average hepatic triglyceride content (%)
Reference values: metabolically normal individual on moderate diet							
Standard parameter values	21.6	2.8	1.2	0.2	4.9	1.2	2.3
Metabolically healthy individual on a very high fat intake diet							
Standard parameter values (untreated)	39.0	2.7	4.1	0.9	5.0	1.2	7.2
Complete suppression of lipogenesis	29.6	2.9	2.9	0.5	5.0	0.9	5.1
Stimulated β-oxidation	17.3	2.5	2.0	0.3	5.0	1.3	3.4
Stimulation of β-oxidation with suppression of DNL	14.3	2.8	1.8	0.3	5.0	0.9	2.9
Severely insulin resistant individual on a raised intake diet							
Standard parameter values (untreated)	26.2	2.2	5.4	3.9	6.7	1.4	8.9
Complete suppression of lipogenesis	12.3	2.6	5.1	0.6	8.5	1.0	7.0
Stimulated β-oxidation	8.9	1.9	3.5	0.5	8.2	1.5	4.8
Stimulation of β-oxidation and suppression of DNL	5.8	2.5	3.0	0.4	8.8	0.9	3.8

form of NAFLD (Figure 3a). If a treatment fails to remove the underlying cause of the disease progression, it will be unable to restore normal function after treatment ceases.

Stimulation of β-Oxidation. Stimulation of β-oxidation (doubling the rate constant), effectively cleared steatosis when simulating both NAFLD caused by high fat intake alone and severely insulin resistant NAFLD patients. In both cases, the liver lipid content was reduced to less than the 5% criterion at which NAFLD is diagnosed (Figure 3a). Furthermore, improvements were predicted in plasma FFA and triglyceride concentrations. However, when stimulating β-oxidation, additional reductions in ATP concentration were predicted, leading to severely reduced values in pericentral cells (Figure 3b). This is due to the allosteric inhibition of glycolysis by increased β-oxidation, along with ATP consumption in increased β-oxidation and lipogenesis. Furthermore, the overactivation of the oxidative phosphorylation pathway was increased, potentially increasing mitochondrial stress. Therefore, despite effectively clearing the underlying cause of disease progression, stimulation of β-oxidation alone is not predicted to provide a safe drug target, and may expedite rather than prevent hepatic damage.

Combination Treatments. A third possibility would be to both suppress the synthesis of fatty acids from acetyl-CoA while stimulating β-oxidation. This is feasible clinically and could be achieved, for example, by inhibiting both cytosolic and mitochondrial forms of acetyl-CoA carboxylase which play a role in lipogenesis and negative regulation of β-oxidation, respectively. The treatment was predicted to effectively clear hepatic triglyceride build-up and reduce the average hepatic FFA concentration, therefore reducing both short-term lipotoxicity and the underlying long-term cause of disease progression (Figure 3a and Table 1). Furthermore ATP concentrations were predicted to be increased to near metabolically normal values and the overactivity of ATP synthesis was prevented (Figure 3b). The only adverse effect to be predicted was an increase in plasma glucose concentration when simulating an insulin resistant individual (Table 1). Therefore, the treatment would need to restore insulin sensitivity rapidly enough to allow the excess glucose to be stored as glycogen, or would need to be accompanied by addition treatments preventing hyperglycaemia.

Drug Screening Potential. The model can be used to screen a range of potential targets and combinations of targets. The two examples reviewed here demonstrate the use of the model to assess the effectiveness of particular drug targets for clearing steatosis in NAFLD and the ability of the model to predict potential adverse effects elsewhere in metabolism. Additionally, the pericentral-specific disruptions to energy metabolism in NAFLD highlights the importance of studying cells across the liver sinusoid. In ongoing work, the model predictions are being tested in cell culture models and it is hoped that the research will help to minimize the future animal work required in drug development.

The model could also be used to determine an optimal choice of target and dose through discrete and continuous optimization techniques so commonly used by Process Systems Engineers today. However the validity of such an approach depends very much on the accuracy of the model in terms of both structure and parameter values. At this stage the use of the model to support or test hypotheses for testing against data is the state of the art as there is considerable uncertainty about the fidelity of the model. In the next section we present the use of a method for exploring the performance of a model to predict hormone levels under uncertainty of the certain key parameters with varied inputs resulting from feeding. This will help determine the limits of behavior of a model outputs under some limited uncertainty conditions since precise model parameter values are difficult if not impossible to obtain.

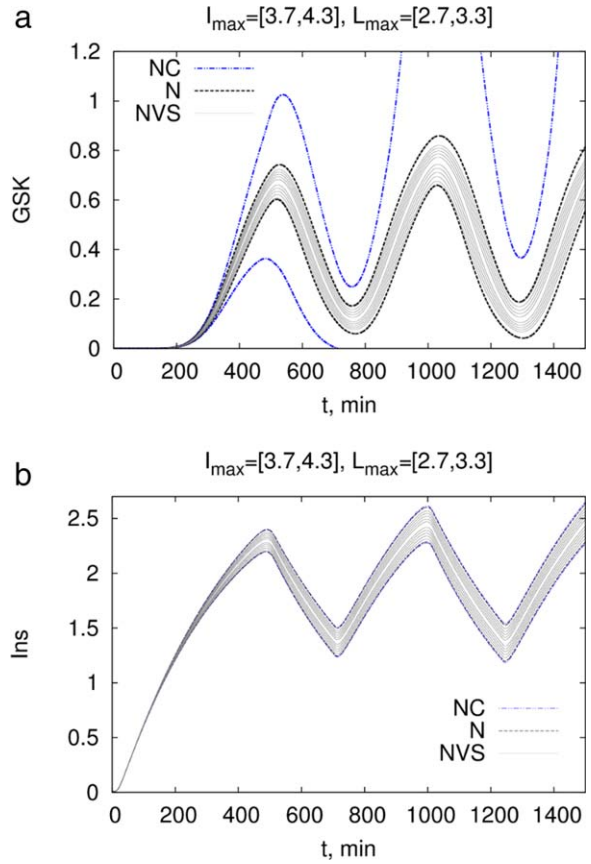

Figure 4. (a) Bounds and non-verified profiles of the GSK state of the Pancreas-Insulin model with uncertainty of [3.7,4.3] in I_{max} and [2.7,3.3] in L_{max}. (b) Bounds and non-verified profiles of the I state of the Pancreas-Insulin model.

[Color figure can be viewed in the online issue, which is available at wileyonlinelibrary.com.]

Range Control Incorporating Uncertain Behavior

Since one of the key functions the liver performs is glucose homeostasis it is important to find ways to make sure the glucose in the blood is between limits to avoid the conditions of hyperglycaemia and hypoglycaemia. It is crucial to remain within safe bounds and not necessary to control glucose or hormone levels to a setpoint. This section discusses an approach based on verified simulation which aims to construct guaranteed upper and lower bounds on the dynamic variables of interest in the liver model. Enszer and Stadtherr[64] have used verified methods in the propagation of uncertainty in physiological models for diabetes and long term starvation exploring also how to account for probability distributions in the uncertainty using p-boxes to bound the distribution. In this article the pancreas-insulin and glucagon receptor models described in Hetherington et al.[32] are taken together for the case study. Two particular model parameters were chosen as uncertain parameters and the model subject to a cycling input to reflect bodily response to feeding cycles. For this we used just a pancreas-insulin and glucagon receptor model rather than the full liver system model given the complexity of the computations required. Interval predictions were obtained using the model explained in the next section.

Interval model for hormone prediction

Pancreas-Insulin Model. The seven compartment model of Hetherington et al.[32] included models for the pancreas, insulin production, and the activation of proteins by glucagon. By coupling these three models we are able to predict the levels of hormones in the system resulting from a glucose stimulus and it is this part of the Hetherington et al. model that has been used here to predict bounds.

Insulin Model. The insulin model describes the activation of glycogen synthase kinase (GSK) in response to the concentration of insulin in the blood (I).

$$\dot{GSK} = \frac{1}{\tau_{GSK}}\left[\Theta_{n_I}(I \cdot I_{scale}, t_I) - GSK\right]$$

$$\tau_{GSK} = 1 \text{ min}, \; t_I = 0.5, n_I = 8, \; I_{scale} = 0.25$$

Pancreas Model. This model describes the release of glucagon (L) or insulin (I) into the blood by the pancreas in response the blood glucose concentration. The model considers a fixed reference level (g_{ref}) of blood glucose (g_B) around which homeostasis should be maintained.

$$\dot{L} = \frac{1}{\tau_L}\left(\Theta_{n_P}\left(h(-x), t_{Lg}\right) - \frac{L}{L_{\max}}\right)$$

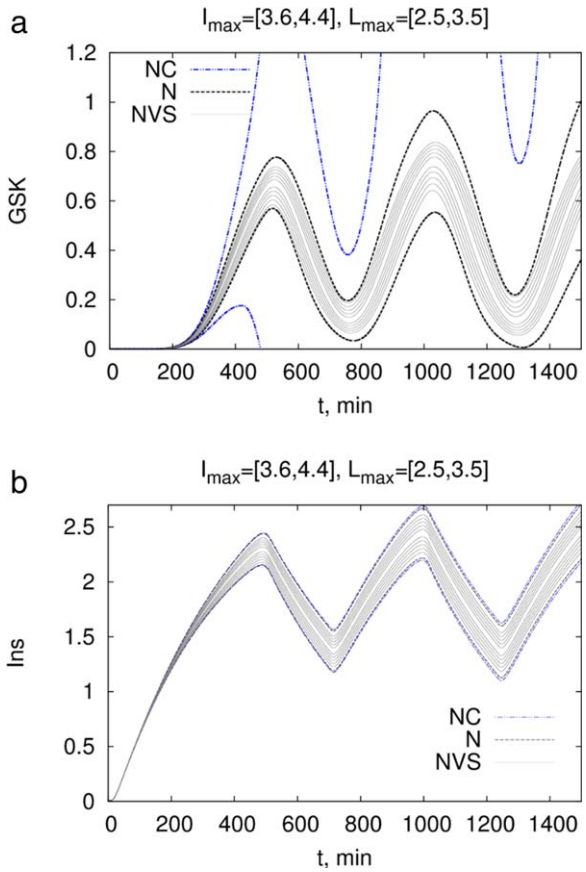

Figure 5. (a) Bounds and non-verified profiles of the GSK state of the Pancreas-Insulin model with larger uncertainty of [3.6,4.4], in I_{max} and [2.5,3.5] in L_{max}. (b) Bounds and non-verified profiles of the I state of the Pancreas-Insulin model.

[Color figure can be viewed in the online issue, which is available at wileyonlinelibrary.com.]

$$\dot{I}=\frac{1}{\tau_I}\left(\Theta_{n_p}\left(h(x),t_{Ig}\right)-\frac{I}{I_{\max}}\right)$$

$$x=\log\left(\frac{g_B g_{scale}}{g_{ref}}\right)$$

$$h(x)=\begin{cases} x \ \ if \ \ x\geq 0, \\ 0 \ \ if \ \ x<0 \end{cases}$$

$$\tau_L=0.25,\ \ \tau_I=\frac{5}{3},\ \ t_{Lg}=0.125,\ \ t_{Ig}=0.25,$$

$$g_{ref}=2.5,\ \ I_{\max}=4,\ \ L_{\max}=3,\ \ n_P=2,$$

$$g_{scale}=5.555556\times 10^{-4}$$

Glucagon Receptor Model. The model describes the activation of G proteins by glucagon which regulates the activation of phospholipase C (PLC). Active PLC produces inositol trisphosphate (IP3) which acts as a second messenger in the mobilization of intracellular calcium. The glucagon receptor model[65] represents a hormone build up in the bloodstream, and is modeled by

$$\dot{R}_r(t)=k_{-1}LR_u-L(t)k_1R_r(t)-k_sR_r(t)+k_rR_s(t)$$

$$\dot{R}_s(t)=k_{sp}LR_p(t)+\mathrm{G}K_{2s}LR_u+k_s(LR_u+R_r(t))-k_rR_s(t)$$

$$\dot{G}(t)=-\mathrm{G}(t)K_{23}LR_u+G_*\left(k_h+\frac{Ca(t)k_{Gdeg,Cal}}{K_{Gdeg,Cal}+G_*}+\frac{PLC_*(t)k_{Gdeg,PLC}}{K_{Gdeg,PLC}+G_*}\right)$$

$$\dot{LR}_p(t)=-k_{sp}LR_p(t)+k_p\left(1+\frac{A_0}{1+B_1{G_*}^{-n_1}}\right)\left(\frac{LR_u}{LR_u+B_2}\right)$$

$$\dot{PLC}_*(t)=k_{PC}G_*-\frac{PLC_*(t)k_{PC,deg}}{K_{PC,deg}+PLC_*(t)}$$

$$G_*=G_0-G_i(t)$$

$$R_0=R_r(t)+R_s+LR_u+LR_p$$

where states G, R_r, R_s, and LR_u and LR_p are the G protein, free receptor, sequestered receptor, ligand-bound receptor, and phosphorylated ligand-bound receptor, respectively. The parameters and initial conditions of the model are

Initial conditions: $R_r(0)=55000$, $R_s(0)=71500$, $G_i(0)=99999$, $LR_p(0)=0$, and $PLC_*(0)=0$

Parameters: $k_{-1}=10$, $k_1=100$, $k_s=5.2*10^{-3}$, $k_{sp}=k_s$, $K_{2s}=2.0*10^{-8}k_s$, $k_r=4.0*10^{-3}$, $K_{23}=1*10^{-7}$, $k_h=2.0*10^{-1}$, $k_{Gdeg,Cal}=1.47*10^3$, $K_{Gdeg,Cal}=3.54*10^1$, $k_{Gdeg,PLC}=2.19*10^3$, $K_{Gdeg,PLC}=5.7$, $k_p=6.5*10^4$, $A_0=3.0$, $B_1=100$, $n_1=1$, $B_2=10^6$, $R_0=5.5*10^4$, $G_0=10^5$, $k_{PC}=6.06*10^{-4}$, $k_{PC,deg}=2.82*10^{-1}$, and $K_{PC,deg}=2.55*10^{-1}$.

Overview of the verified method

To construct bounds on the dynamic variables of the pancreas-insulin and glucagon receptor models a verified method has been used (see, e.g., Lin and Stadtherr[66]). Verified methods represent an option for managing uncertainty in a rigorous way in which the truncation and round off errors in the numerical computations are accounted for. Verified methods can suffer from overestimation which can cause the computed bounds to blow up and tend to $\pm\infty$. However there are mechanisms to control the generation of the overestimation using methods such as verified integrations based on Taylor models,[67] McCormick relaxations,[68] ellipsoidal calculus,[69] other verified enclosures,[70] and the use of interval contractors.[71]

The bounding method used in this article relies on an interval Taylor series method[72] with an interval contractor based on the Newton and Gauss/Seidel methods[73] for overestimation reduction.

Interval Taylor Series Method with Newton/Gauss-Seidel Contractor. The interval Taylor series with Newton/Gauss-Seidel contractor method (ITS-N) used in this article consists of two stages. The first stage is the validation of existence and uniqueness of a solution in which also a suitable a priori enclosure and a time step are obtained. The second stage involves the computation of a tighter enclosure in which a high order Taylor series is used to refine the solution obtained in the first stage. When the contractor is not used the method is simply called interval Taylor series (ITS).

First Stage. In the first stage a validation of existence and uniqueness is carried out using the High Order Enclosure (HOE) approach.[74] An appropriate time step h_j and an a priori enclosure $\tilde{\boldsymbol{Y}}_j$ need to be obtained and they satisfy:

$$\tilde{\boldsymbol{Y}}_j=\boldsymbol{Y}_j+\sum_{i=1}^{k-1}\left[0,h_j\right]^i\boldsymbol{f}^{[i]}\left(\boldsymbol{Y}_j,\boldsymbol{\Theta}\right)+\left[0,h_j\right]^k\boldsymbol{f}^{[k]}\left(\tilde{\boldsymbol{Y}}_j^0,\boldsymbol{\Theta}\right)\subseteq\tilde{\boldsymbol{Y}}_j^0$$

where k is the order of the Taylor expansion, $\boldsymbol{f}^{[i]}$ are the Taylor, $\boldsymbol{Y}_j$ is the vector of tight enclosures of the solutions with ranges in $\tilde{\boldsymbol{Y}}_j^0$ and $\boldsymbol{\Theta}$ is the vector of (possibly uncertain) parameters.

Second Stage. The second stage involves the computation of a tighter enclosure $\boldsymbol{Y}_{j+1}$. The tight enclosure satisfies

$$\boldsymbol{Y}_{j+1}=\overbrace{\hat{\boldsymbol{y}}_j+\sum_{i=1}^{k-1}h_j^i\boldsymbol{f}^{[i]}\left(\hat{\boldsymbol{y}}_j,\hat{\boldsymbol{\theta}}\right)}^{\boldsymbol{u}_{j+1}}+\overbrace{\left\{\boldsymbol{I}+\sum_{i=1}^{k-1}h_j^i\frac{\partial\boldsymbol{f}^{[i]}}{\partial\boldsymbol{y}}\left(\boldsymbol{Y}_j,\boldsymbol{\Theta}\right)\right\}}^{\boldsymbol{S}_{j+1}^{y}}\left(\boldsymbol{Y}_j-\hat{\boldsymbol{y}}_j\right)+\underbrace{\sum_{i=0}^{k-1}h_j^i\frac{\partial\boldsymbol{f}^{[i]}}{\partial\boldsymbol{\theta}}\left(\boldsymbol{Y}_j,\boldsymbol{\Theta}\right)}_{\boldsymbol{S}_{j+1}\theta}\left(\boldsymbol{\Theta}-\hat{\boldsymbol{\theta}}\right)+\underbrace{h_j^k\boldsymbol{f}^{[k]}\left(\tilde{\boldsymbol{Y}}_j,\boldsymbol{\Theta}\right)}_{\boldsymbol{Z}_{j+1}}$$

where $\boldsymbol{I}$ is the identity matrix, and $\hat{\boldsymbol{y}}_j$ and $\hat{\boldsymbol{\theta}}$ are the midpoints of $\boldsymbol{Y}_j$ and $\boldsymbol{\Theta}$, respectively.

The interval matrix-vector product $\boldsymbol{S}_{j+1}^{y}\left(\boldsymbol{Y}_j-\hat{\boldsymbol{y}}_j\right)$ in the previous equation is known to be one of the main contributors of the wrapping effect in interval arithmetic. Because of this, a number of methods have been developed to try to avoid the direct evaluations of this matrix-vector product.[72] In this article the QR factorization technique devised by Lohner[75] is used in the interval Taylor series method.

In this work the Newton with Gauss-Seidel nonlinear contractor to reduce the overestimation has been used.[71] For more details about contractors see Jaulin.[73] The algorithm for this method has been written in C++ and the libraries FADBAD++[76] and Profil/Bias[77] have been used for the automatic differentiation and the interval type, respectively.

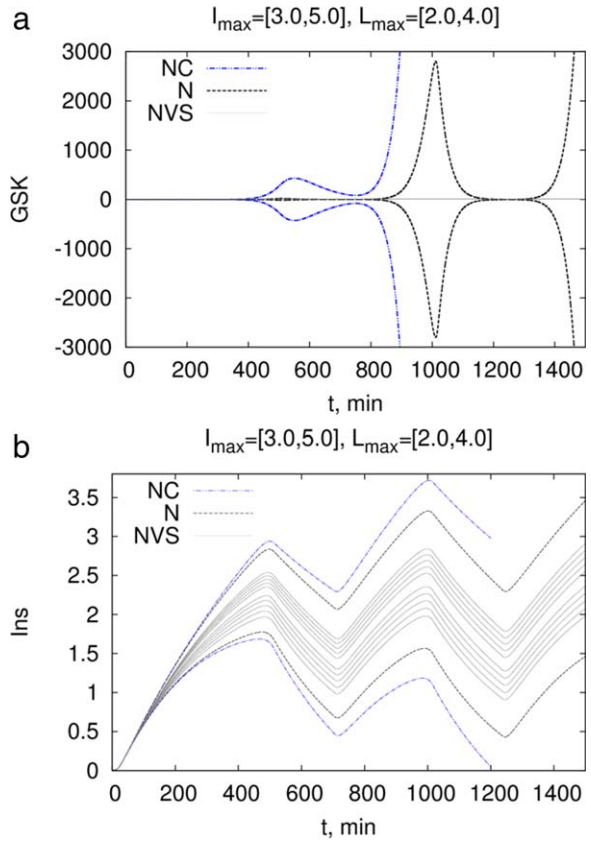

Figure 6. (a) Bounds and non-verified profiles of the GSK state of the Pancreas-Insulin model with 25% in I_{max} and 33% in L_{max}. (b) Bounds and non-verified profiles of the I state of the Pancreas-Insulin model.

[Color figure can be viewed in the online issue, which is available at wileyonlinelibrary.com.]

Control under uncertainty using interval analysis bounding glucose concentration

The response of the models under uncertainty using a verified method is studied in the following numerical experiments. The verified method described in the previous subsection with no contractor (ITS) and with contractor (ITS-N) are used in the pancreas-insulin model. Then the method with contractor and VSPODE,[78] a state of the art solver, are used to compute bounds in the glucagon receptor model with different uncertain amounts.

Pancreas Insulin Model Numerical Experiments. Uncertain amounts were introduced in the pancreas-insulin model to evaluate the effectiveness of the ITS-N and ITS methods in accounting for uncertainty to see if they are able to provide reasonable estimates of bounds for the output variables. In the model two uncertain amounts were used and simulations were carried out varying the level of uncertainty. The parameters I_{max} and L_{max} were chosen as they define the maximum possible blood concentrations of glucagon and insulin safely permissible. In this way, if the model can manage uncertainty in these parameters then it could be used in studies involving different patients requiring different (tuning) parameters for the maximum levels of glucagon and insulin.

In a first set of numerical experiments an uncertainty of $I_{max} = [3.7,4.3]$, $L_{max} = [2.7,3.3]$ was introduced. The profiles of the variables GSK and I (insulin) can be seen in Figures 4a, b. To represent an approximation of the solution in which uncertainty has been introduced, sample trajectories that span the uncertain amount considered (solid grey lines) have been included in Figures 4a, b. Two simulations were carried out one with the ITS method (dot-dot-dashed line) and one with the ITS-N (dashed black line), these are shown in the figures as well. The solution provided by the ITS-N is very tight as the bounds approach closely to the set of approximate solutions (solid grey lines). The uncertainty of the bounds of the three states at the final time ($t_f = 1500$ min) is $GSK(t_f) = [0.5546,0.8144]$, $L(t_f) = [0.6345,0.8363]$ and $I(t_f) = [2.2865,2.6349]$. Conversely, the solution provided by the ITS method is more conservative as there is a significant distance between the approximate solutions and the bounds. The uncertainty at final time is $GSK(t_f) = [-1.4818,2.8508]$, $L(t_f) = [0.6258,0.8451]$, and $I(t_f) = [2.2718,2.6496]$. The uncertainty is similar in the bounds except in *GSK* where the wideness of the bounds (distance between the upper and lower bound) grows from 0.2596 to 4.3325.

A second numerical experiment was carried out in a similar fashion and the uncertainty in the parameters $I_{max} = [3.6,4.4]$, $L_{max} = [2.5,3.5]$ was used (Figures 5a, b). The uncertainty of the bounds at final time using the ITS-N was $GSK(t_f) = [0.3629,1.0061]$, $L(t_f) = [0.5324,0.9385]$, and $I(t_f) = [2.2106,2.7108]$. Using the ITS method the bounds obtained at final time were $GSK(t_f) = [-8.3993,9.7684]$, $L(t_f) = [0.4951,0.9757]$, and $I(t_f) = [2.1794,2.7420]$. As in the previous case there was significant difference in the wideness between the bounds computed by the ITS (with wideness of 18.1677) and the ITS-N (with wideness of 0.6431) methods only in the *GSK* variable.

Finally, to take the method to the limit a third case of uncertainties of $\pm 25\%$ in I_{max} and $\pm 33\%$ in L_{max} ($I_{max} = [3.0,5.0]$, $L_{max} = [2.0,4.0]$) was considered (Figures 6a, b). Both of the methods computed conservative bounds in the three state variables but particularly in GSK. In the case of the ITS method the simulation had to be stopped (around t = 1200 min) due to excessive wideness whereas in the ITS-N method the uncertainty of GSK at final time was [−8256,8256]. The other state variables could be enclosed by both of the methods with ITS-N being tighter as shown in Figure 6b. The uncertainties of variable insulin I at intermediate time $t_i = 1200$ min of the ITS and ITS-N methods are [0.5682,2.4597] and [0.0500,2.9782], respectively.

The ITS method computed tight bounds only in the L and I state variables but when it came to bound the GSK state variable the ITS-N method was much tighter as observed in the width of the GSK bounds. Comparing the bounds of the GSK variable at final time using the ITS and ITS-N methods, the first one turned out to be approximately 16 times wider than the second one in the first set of experiments and 30 times in the second set of experiments. Unlike the ITS-N method the ITS method did not complete the simulations in the third set of experiments.

Glucagon Receptor Model Numerical Experiments. The numerical experiments in the glucagon receptor model address the introduction of uncertainty in the higher dimensional system using VSPODE. The ITS and ITS-N methods are only able to address a small amount of uncertainty in one parameter in this case study.

An uncertainty of $B_1 = [98.8,101.2]$ was introduced in the model and the ITS-N method and VSPODE were used to compute bounds (Figure 7). A disturbance was also introduced in

the form of a step change (at time t = 550 s) in the input corresponding to g_B, the concentration of blood glucose. The bounds at final time (800 s) using the ITS-N (dashed black line) and VSPODE (dot-dot-dashed line) methods for the R_s state were [72272.70,72279.80] and [72275.40,72277.06], respectively. VSPODE computes tighter bounds with a width at final time of 1.66 whereas ITS-N obtains a width of 7.1.

Bounds for systems biology models are more useful when significant amounts of uncertainty can be accounted for and tight bounds can be computed. Unfortunately the ITS-N method is still not capable of addressing this problem. In the next experiment a Taylor models based method (VSPODE) is used to compute bounds for the Glucagon receptor model with ±2% of uncertainty in three parameters (Figure 8). The parameters are $B_1 = [98,102]$, $k_h = [0.196,0.204]$, and $k_s = [0.005096,0.005304]$. These parameters represent key rates of reaction of some of the receptors in the model. Furthermore, a step change in the input of blood glucose has been performed at time t = 550 s to see the tightness of the bounds when there is a disturbance in the system. As in the previous cases Figure 8 presents sample non-verified solutions (NVS) together with the computed bounds.

The use of verified methods in systems biology is a useful tool to address uncertainty of a dynamic system in a guaranteed way. The ITS method computed very conservative bounds in all experiments in the GSK variable, much greater than those obtained with the ITS-N. The ITS-N method proved to be able to provide bounds in an effective way in the first two sets of experiments. In the third case when the uncertainty grew larger than ±25% in the parameters the bounds were again highly conservative so clearly there is still a need for improvement since the introduction of larger uncertain amounts is still a difficult task. The results for the glucagon receptor model using VSPODE and ITS-N show that the Taylor model method is still one of the best for computing bounds for higher dimensional models as they resulted tighter bounds than with ITS-N. In a second set of experiments VSPODE handled ±2% of uncertainty in the three parameters plus a disturbance in the form of a step change input. These results could be extended to use the probabilistic approach proposed by Enszer and Stadtherr.[64] However, the variables where uncertainties were chosen to explore the sensitivity of the enclosure ranges cannot been directly measured. A more

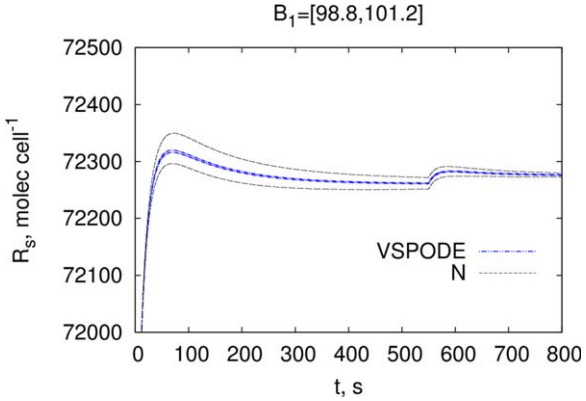

Figure 7. Bounds for the R_s state of the Glucagon receptor model with uncertainty of [98.8, 101.2] in B_1.

[Color figure can be viewed in the online issue, which is available at wileyonlinelibrary.com.]

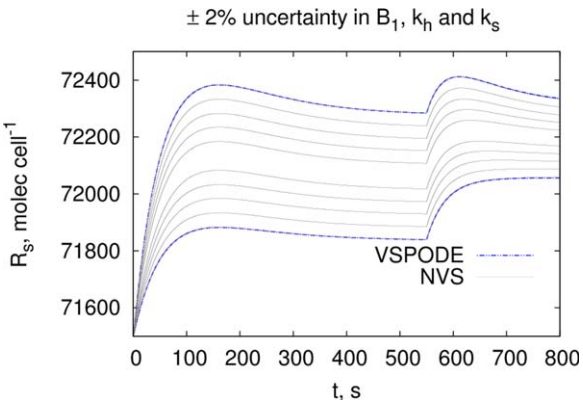

Figure 8. Bounds for the R_s state of the Glucagon receptor model with uncertainty in three parameters: B_1, k_h, and k_s.

[Color figure can be viewed in the online issue, which is available at wileyonlinelibrary.com.]

suitable approach to explore probabilistic behavior would be to use ranges of distributions of key clinical variables such as glucose and insulin and to determine possible ranges of key insulin resistance variables in the whole composite model.[32]

Conclusions

We have aimed to demonstrate a role that Process Systems Engineers can have in medical problems using two particular approaches. This work has focussed on the body's "chemical factory," the liver system, which plays a central role in regulating the level of glucose in the blood stream. Distributed system modeling is a new development in modeling liver behavior but necessary to be able to predict and eventually optimize drug behavior. Regulation of glucose between strict bounds is vital for the health of patients but requires that we are able to make reasonable predictions with uncertainty in the parameters and this continues to be a challenge.

In this domain systems are very complex and data can be either very comprehensive based on *in vitro* experiments or sparse and inaccurate from *in vivo* studies of patients. Modellers from the Process Systems community (Hangos and Cameron[36]) and the Systems Biology/Medicine community (Batzel et al.[78]) agree that models should be designed for a specific purpose and care taken when used beyond this original objective. With a clear objective in mind it becomes tractable to include the phenomena and metabolic processes which are known to be directly relevant to the purpose. Heldt et al.[79] discuss in some detail the choice of model structure, methods for identification and parameter estimation, and model order reduction to achieve the best possible model fidelity. Our experience has led us to developing models from key phenomena able to predict known results and building on known verified models, identified at each stage with best available data from experiments and patients (recognising that data is often not of high quality), and gradually extended to involve new phenomena as needed. This is in line with Noble's[10] middle-out approach starting from well understood phenomena and building out. This results in predicting trends accurately and often, although by no means always, reasonably accurate predictions of output variables. However, this is a complex topic that requires a more extended discussion.

For the Process Systems role to grow in the medical domain requires us to introduce our students to this area and to forge

collaborations with medical researchers and clinicians. Sargent[1] commented on the difficulty of covering a wide range of topics while ensuring competence in our tools and methods. Through collaboration with domain experts our community can help solve some of the challenging problems in Systems Medicine and contribute in this way to human wellbeing.

Literature Cited

1. Sargent R. Process systems engineering: a retrospective view with questions for the future. *Comput Chem Eng*. 2005;29(6):1237–1241.
2. Sargent RWH. My contribution to broadening the base of chemical engineering. *Annu Rev Chem Biomol*. 2011;2:1–7.
3. Bogle IDL. Recent developments in process systems engineering as applied to medicine. *Curr Opin Chem Eng*. 2012;1(4):453–458.
4. Bogle IDL, Allen R, Sumner T. The role of computer aided process engineering in physiology and clinical medicine. *Comput Chem Eng*. 2010;34(5):763–769.
5. Stokes CL. Biological systems modeling: powerful discipline for biomedical e-R&D. *AICHE J*. 2000;46(3):430–433.
6. Androulakis IP. A chemical engineer's perspective on health and disease. *Comput Chem Eng*. 2014;71:665–671.
7. Ierapetritou MG, Georgopoulos PG, Roth CM, Androulakis IP. Tissue-level modeling of xenobiotic metabolism in liver: an emerging tool for enabling clinical translational research. *Cts-Clin Transl Sci*. 2009;2(3):228–237.
8. Linninger AA. Biomedical systems research-New perspectives opened by quantitative medical imaging. *Comput Chem Eng*. 2012; 36:1–9.
9. Bogle IDL, Jalan R, Shephard E, Seymour R, Finkelstein A, Sumner T, Warner A. Systems biology of the liver. In: R.A. Myers, editor. *Encyclopedia of Molecular Cell Biology and Molecular Medicine*. Weinheim, Wiley, 2012:539–561.
10. Noble D. Modelling the heart: insights, failures and progress. *BioEssays*. 2002;24(12):1155–1163.
11. Glynn P, Unudurthi SD, Hund TJ. Mathematical modeling of physiological systems: an essential tool for discovery. *Life Sci*. 2014; 111(1–2):1–5.
12. Mishra L. The 21st century hepatologist and a systems biology based approach to liver diseases. *Hepatology*. 2008;48(6):1731–1733.
13. Geletu ALP. Recent developments in computational approaches to optimization under uncertainty and application in process systems engineering. *ChemBioEng Rev*. 2014;1(4):170–190.
14. Sun A, Jiang Y, Wang X, Liu Q, Zhong F, He Q, Sun A, Jiang Y, Wang X, Liu Q, Zhong F, He Q, Guan W, Li H, Sun Y, Shi L, Yu H, Yang D, Xu Y, Song Y, Tong W, Li D, Lin C, Hao Y, Geng C, Yun D, Zhang X, Yuan X, Chen P, Zhu Y, Li Y, Liang S, Zhao X, Liu S, He F. Liverbase: a comprehensive view of human liver biology. *J Proteome Res*. 2010;9(1):50–58.
15. Almeda-Valdes P, Cuevas-Ramos D, Aguilar-Salinas CA. Metabolic syndrome and non-alcoholic fatty liver disease. *Ann Hepatol*. 2009; 8(Suppl 1):S18–S24.
16. Manchanayake J, Chitturi S, Nolan C, Farrell GC. Postprandial hyperinsulinemia is universal in non-diabetic patients with nonalcoholic fatty liver disease. *J Gastroen Hepatol*. 2011;26(3):510–516.
17. Jungermann K, Katz N. Functional specialization of different hepatocyte populations. *Phys Rev*. 1989;69(3):708–764.
18. Balakrishnan NP, Rangaiah GP, Samavedham L. Review and analysis of blood glucose (BG) models for type 1 diabetic patients. *Ind Eng Chem Res*. 2011;50(21):12041–12066.
19. Li Z, Chan C. Systems biology for identifying liver toxicity pathways. *BMC Proc*. 2009;3(Suppl 2):S2.
20. Subramanian K, Raghavan S, Rajan Bhat A, Das S, Bajpai Dikshit J, Kumar R, Narasimha MK, Nalini R, Radhakrishnan R, Raghunathan S. A systems biology based integrative framework to enhance the predictivity of in vitro methods for drug-induced liver injury. *Exp Opin Drug Safe*. 2008;7(6):647–662.
21. Galvanin F, Barolo M, Macchietto S, Bezzo F. Optimal design of clinical tests for the identification of physiological models of type 1 diabetes mellitus. *Ind Eng Chem Res*. 2009;48(4):1989–2002.
22. Finan DA, Palerm CC, Doyle FJ, Seborg DE, Zisser H, Bevier WC, Jovanovič, L. Effect of input excitation on the quality of empirical dynamic models for type 1 diabetes. *AICHE J*. 2009;55(5):1135–1146.
23. Zavitsanou S, Panoskaltsi N, Mantalaris A, Georgiadis MC, Pistikopoulos EN. Modelling of the Insulin delivery system for patients with type 1 diabetes mellitus. *Comput-Aided Chem Eng*. 2011;29:1500–1504.
24. Semizer E, Yuceer M, Atasoy I, Berber R. Comparison of control algorithms for the blood glucose concentration in a virtual patient with an artificial pancreas. *Chem Eng Res Des*. 2012;90(7):926–937.
25. Percival MW, Dassau E, Zisser H, Javanovic L, Doyle FJ. Practical approach to design and implementation of a control algorithm in an artificial pancreatic beta cell. *Ind Eng Chem Res*. 2009;48(13):6059–6067.
26. Liu WJ, Hsin CC, Tang FS. A molecular mathematical model of glucose mobilization and uptake. *Math Biosci*. 2009;221(2):121–129.
27. Liu WJ, Tang FS. Modeling a simplified regulatory system of blood glucose at molecular levels. *J Theor Biol*. 2008;252(4):608–620.
28. Cardenas ML, Goldbeter A. The glucose-induced switch between glycogen phosphorylase and glycogen synthase in the liver: Outlines of a theoretical approach. *J Theor Biol*. 1996;182(3):421–426.
29. Klingmüller U, Bauer A, Bohl S, Nickel PJ, Breitkopf K, Dooley S, Zellmer S, Kern C, Merfort I, Sparna T, Donauer J, Walz G, Geyer M, Kreutz C, Hermes M, Götschel F, Hecht A, Walter D, Egger L, Neubert K, Borner C, Brulport M, Schormann W, Sauer C, Baumann F, Preiss R, MacNelly S, Godoy P, Wiercinska E, Ciuclan L, Edelmann J, Zeilinger K, Heinrich M, Zanger UM, Gebhardt R, Maiwald T, Heinrich R, Timmer J, von Weizsäcker F, Hengstler JG. Primary mouse hepatocytes for systems biology approaches: a standardized in vitro system for modelling of signal transduction pathways. *IEE P Syst Biol*. 2006;153(6):433–447.
30. Wu M, Yang XR, Chan C. A dynamic analysis of IRS-PKR signaling in liver cells: a discrete modeling approach. *Plos One*. 2009; 4(12):e8040.
31. Kim J, Saidel GM, Cabrera ME. Multi-scale computational model of fuel homeostasis during exercise: effect of hormonal control. *Ann Biomed Eng*. 2007;35(1):69–90.
32. Hetherington J, Sumner T, Seymour RM, Li L, Varela Rey V, Yamaji S, Saffrey P, Margoninski O, Bogle IDL, Finkelstein A, Warner A. A composite computational model of liver glucose homeostasis. I. Building the composite model. *J Roy Soc*. 2012;9(69): 689–700.
33. Sumner T, Hetherington J, Seymour RM, Li L, Varela Rey M, Yamaji S, Saffrey P, Margoninski O, Bogle IDL, Finkelstein A, and Warner A. A composite computational model of liver glucose homeostasis. II. Exploring system behaviour. *J Roy Soc*. 2012;9(69):701–706.
34. Saffrey P, Margoninski O, Hetherington J, Varela Rey M, Yamaji S, Bogle IDL, Finkestein A, Warner A. End-to-end information management for systems biology. In: Priami C, editor. *Transactions on Computational Systems Biology VIII*. Heidelberg: Springer-Verlag Berlin, 2007:77–91.
35. Sumner T, Shephard E, Bogle ID. A methodology for global-sensitivity analysis of time-dependent outputs in systems biology modelling. *J Roy Soc*. 2012;9(74):2156–2166.
36. Hangos K, Cameron IT. *Process modeling and model analysis*, 1st ed. Academic Press, Cambridge MA, 2001.
37. Jungermann K, Kietzmann T. Role of oxygen in the zonation of carbohydrate metabolism and gene expression in liver. *Kidney Int*. 1997;51(2):402–412.
38. Chalasani N, Wilson L, Kleiner DE, Cummings OW, Brunt EM, Ünalp A, and for the NASH Clinical Research Network. Relationship of steatosis grade and zonal location to histological features of steatohepatitis in adult patients with non-alcoholic fatty liver disease. *J Hepatol*. 2008;48(5):829–834.
39. Brunt EM. Pathology of fatty liver disease. *Modern pathology: an official journal of the United States and Canadian Acad Pathol*. 2007;20(Suppl 1):S40–S48.
40. Hijmans BS, Grefhorst A, Oosterveer MH, Groen AK. Zonation of glucose and fatty acid metabolism in the liver: mechanism and metabolic consequences. *Biochimie* 2014;96:121–129.
41. Abdelmalek MF, Diehl AM. Nonalcoholic fatty liver disease as a complication of insulin resistance. *Med Clin N Am*. 2007;91(6): 1125–1149.
42. Ashworth W, Davies N, Bogle IDL. A computational model of hepatic energy metabolism: understanding zonated damage and steatosis in NAFLD. Submitted—Under Review. 2016.
43. Ohno H, Naito Y, Nakajima H, Tomita M. Construction of a biological tissue model based on a single-cell model: a computer simulation of metabolic heterogeneity in the liver lobule. *Artificial Life*. 2008; 14(1):3–28.

44. Konig M, Bulik S, Holzhutter HG. Quantifying the contribution of the liver to glucose homeostasis: a detailed kinetic model of human hepatic glucose metabolism. *PLOS Comput Biol*. 2012;8(6):e1002577.
45. Daly ME, Vale C, Walker M, Littlefield A, Alberti KG, Mathers JC. Acute effects on insulin sensitivity and diurnal metabolic profiles of a high-sucrose compared with a high-starch diet. *Am J Clin Nutr*. 1998;67(6):1186–1196.
46. Szczepaniak LS, Nurenberg P, Leonard D, Browning JD, Reingold JS, Grundy S, Hobbs HH, Dobbins RL. Magnetic resonance spectroscopy to measure hepatic triglyceride content: prevalence of hepatic steatosis in the general population. *Am J Physiol Endocrinol Metabol*. 2005;288(2):E462–E468.
47. Shimomura I, Bashmakov Y, Horton JD. Increased levels of nuclear SREBP-1c associated with fatty livers in two mouse models of diabetes mellitus. *J Biol Chem*. 1999;274(42):30028–30032.
48. Browning JD, Horton JD. Molecular mediators of hepatic steatosis and liver injury. *J Clin Invest*. 2004;114(2):147–152.
49. Sindelka G, Skrha J, Prazny M, Haas T. Association of obesity, diabetes, serum lipids and blood pressure regulates insulin action. *Physiol Res*. 2002;51(1):85–91.
50. Berndt J, Kovacs P, Ruschke K, Klöting N, Fasshauer M, Schön MR, Körner A, Stumvoll M, Blöher M. Fatty acid synthase gene expression in human adipose tissue: association with obesity and type 2 diabetes. *Diabetologia* 2007;50(7):1472–1480.
51. Hammad ES, Striffler JS, Cardell RR, Jr. Morphological and biochemical observations on hepatic glycogen metabolism in mice on a controlled feeding schedule. II. Streptozotocin-diabetic mice. *Dig Dis Sci*. 1982;27(8):692–700.
52. Henly DC, Phillips JW, Berry MN. Suppression of glycolysis is associated with an increase in glucose cycling in hepatocytes from diabetic rats. *J Biol Chem*. 1996;271(19):11268–11271.
53. Brehm A, Krssak M, Schmid AI, Nowotny P, Waldhausl W, Roden M. Increased lipid availability impairs insulin-stimulated ATP synthesis in human skeletal muscle. *Diabetes* 2006;55(1):136–140.
54. Schmid AI, Szendroedi J, Chmelik M, Krssak M, Moser E, Roden M. Liver ATP synthesis is lower and relates to insulin sensitivity in patients with type 2 diabetes. *Diabetes Care* 2011;34(2):448–453.
55. Bugianesi E, Gastaldelli A, Vanni E, Gambino R, Cassader M, Baldi S, Ponti V, Pagano G, Ferrannini E, Rizzetto M. Insulin resistance in non-diabetic patients with non-alcoholic fatty liver disease: sites and mechanisms. *Diabetologia* 2005;48(4):634–642.
56. Alves TC, Befroy DE, Kibbey RG, Kahn M, Codella R, Carvalho RA, Falk Petersen K, Shulman GI. Regulation of hepatic fat and glucose oxidation in rats with lipid-induced hepatic insulin resistance. *Hepatology* 2011;53(4):1175–1181.
57. Roden M. Mechanisms of disease: hepatic steatosis in type 2 diabetes—pathogenesis and clinical relevance. *Nat Clin Pract Endoc*. 2006;2(6):335–348.
58. Wellen KE, Hotamisligil GS. Inflammation, stress, and diabetes. *J Clin Invest*. 2005;115(5):1111–1119.
59. Gusdon AM, Song KX, Qu S. Nonalcoholic fatty liver disease: pathogenesis and therapeutics from a mitochondria-centric perspective. *Oxid Med Cell Longev*. 2014:1–20
60. Serviddio G, Bellanti F, Tamborra R, Rollo T, Romano AD, Giudetti AM, Capitano N, Petrella A, Vendemiale G, Altomare E. Alterations of hepatic ATP homeostasis and respiratory chain during development of non-alcoholic steatohepatitis in a rodent model. *Eur J Clin Invest*. 2008;38(4):245–252.
61. Serviddio G, Bellanti F, Tamborra R, Rollo T, Capitanio N, Romano AD, Sarastre J, Vendemiale G, Altomare E. Uncoupling protein-2 (UCP2) induces mitochondrial proton leak and increases susceptibility of non-alcoholic steatohepatitis (NASH) liver to ischaemia-reperfusion injury. *Gut* 2008;57(7):957–965.
62. Garciaruiz C, Colell A, Morales A, Kaplowitz N, Fernandezcheca JC. Role of oxidative stress generated from the mitochondrial electron-transport chain and mitochondrial glutathione status in loss of mitochondrial-function and activation of transcription factor nuclear factor-kappa-B—studies with isolated-mitochondria and rat hepatocytes. *Mol Pharmacol*. 1995;48(5):825–834.
63. Hensley K, Kotake Y, Sang H, Pye QN, Wallis GL, Kolker LM, Tabatabaie T, Stewart CA, Konishi Y, Nakae D, Floyd RA. Dietary choline restriction causes complex I dysfunction and increased H2O2 generation in liver mitochondria. *Carcinogenesis* 2000;21(5):983–989.
64. Enszer JA, Stadtherr MA. Verified solution and propagation of uncertainty in physiological models. *Reliable Comput*. 2011;15:168–178.
65. Hetherington J, Bogle IDL, Saffrey P, Margoninski O, Li L, Varela Rey M, Yamaji S, Baigent S, Ashmore J, Page K, Seymour RM, Finkelstein A, Warner A. Addressing the challenges of multiscale model management in systems biology. *Comput Chem Eng*. 2007;31(8):962–979
66. Lin Y, Stadtherr MA. Validated solutions of initial value problems for parametric ODEs. *Appl Numer Math*. 2007;57/10:1145–1162
67. Makino K, Berz M. Taylor models and other validated functional inclusion methods. *Int J Pure Appl Math*. 2003;4(4):379–456.
68. Sahlodin AM, Chachuat B. Discretize-then-relax approach for convex/concave relaxations of the solutions of parametric ODEs. *Appl Numer Math*. 2011;61(7):803–820.
69. Houska B, Villanueva ME, Chachuat B. A validated integration algorithm for nonlinear ODEs using Taylor models and ellipsoidal calculus. IEEE 52nd Annual Conference on Decision and Control, Florence, 2013:484–489.
70. Rauh A, Auer E. Verified simulation of ODEs and DAEs in ValEncIA-IVP. *Reliable Comput*. 2011;15(4):370–381.
71. Perez-Galvan C, Bogle IDL. Comparison between interval methods to solve initial value problems in chemical process design. In: Klemes JJ, Varbanov PS, Liew PY, editors. 24th European Symposium on Computer Aided Process Engineering, 2014:1405–1410.
72. Nedialkov NS, Jackson KR, Corliss GF. Validated solutions of initial value problems for ordinary differential equations. *Appl Math Comput*. 1999;105(1):21–68.
73. Jaulin L. *Applied interval analysis: with examples in parameter and state estimation, robust control and robotics*. Springer Science & Business Media, London, 2001.
74. Nedialkov NS, Jackson KR, Pryce JD. An effective high-order interval method for validating existence and uniqueness of the solution of an IVP for an ODE. *Reliable Comput*. 2001;7(6):449–465.
75. Lohner RJ. Computation of guaranteed enclosures for the solutions of ordinary initial and boundary value problems. In Cash JR and Gladwell I, editors. *Computational Ordinary Differential Equations. Institute of Mathematics and its Applications Conference Series 39*. Oxford University Press, 1992:425–436.
76. Bendtsen C, Stauning O. FADBAD, a flexible C++ package for automatic differentiation. Department of Mathematical Modelling, Technical University of Denmark, 1996.
77. Knüppel O. PROFIL/BIAS—a fast interval library. *Computing* 1994;53(3–4):277–287.
78. Batzel J, Bachar M, Kappel F, editors. *Mathematical Modelling and Validation in Physiology: Applications to the Cardiovascular and Respiratory Systems. Lecture Notes in Mathematics 2064*. Springer, Berlin, 2013.
79. Heldt T, Verghese GC, Mark RG. Mathematical modeling of physiological systems. In: Batzel J, Bachar M, Kappel F, editors. *Mathematical Modelling and Validation in Physiology*. Springer, Berlin, 2014:21–38.

Manuscript received Feb. 12, 2016, and revision received Apr. 21, 2016.